

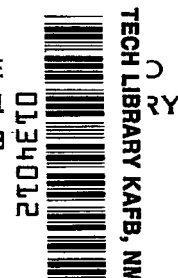
NASA
TN
D-8317
v.1
c.1

NASA TECHNICAL NOTE



NASA TN D-8049

LOAN COPY: RE
AFWL TECHNICAL
KIRTLAND AFB



ISOTHERMAL ELASTOHYDRODYNAMIC LUBRICATION OF POINT CONTACTS

I - Theoretical Formulation

Bernard J. Hamrock and Duncan Dowson

Lewis Research Center

Cleveland, Ohio 44135

NATIONAL AERONAUTICS AND SPACE ADMINISTRATION • WASHINGTON, D. C. • AUGUST 1975





0134012

1. Report No. NASA TN D-8049		2. Government Accession No.	
4. Title and Subtitle ISOTHERMAL ELASTOHYDRODYNAMIC LUBRICATION OF POINT CONTACTS I - THEORETICAL FORMULATION		5. Report Date August 1975	
		6. Performing Organization Code	
7. Author(s) Bernard J. Hamrock, Lewis Research Center; and Duncan Dowson, Leeds University, Leeds, England		8. Performing Organization Report No. E-8295	
9. Performing Organization Name and Address Lewis Research Center National Aeronautics and Space Administration Cleveland, Ohio 44135		10. Work Unit No. 505-04	
		11. Contract or Grant No.	
12. Sponsoring Agency Name and Address National Aeronautics and Space Administration Washington, D. C. 20546		13. Type of Report and Period Covered Technical Note	
		14. Sponsoring Agency Code	
15. Supplementary Notes			
16. Abstract <p>The isothermal elastohydrodynamic lubrication (EHL) of a point contact was analyzed numerically by simultaneously solving the elasticity and Reynolds equations. In the elasticity analysis the contact zone was divided into equal rectangular areas, and it was assumed that a uniform pressure was applied over each area. In the numerical analysis of the Reynolds equation, a phi analysis (where phi is equal to the pressure times the film thickness to the 3/2 power) was used to help the relaxation process. The EHL point contact analysis is applicable for the entire range of elliptical parameters and is valid for any combination of rolling and sliding within the contact.</p>			
17. Key Words (Suggested by Author(s)) Elastohydrodynamic lubrication Bearings Gear Contact between solids		18. Distribution Statement Unclassified - unlimited STAR Category 37 (rev.)	
19. Security Classif. (of this report) Unclassified	20. Security Classif. (of this page) Unclassified	21. No. of Pages 31	22. Price* \$3.75

ISOTHERMAL ELASTOHYDRODYNAMIC LUBRICATION OF POINT CONTACTS

I - THEORETICAL FORMULATION

by Bernard J. Hamrock and Duncan Dowson*

Lewis Research Center

SUMMARY

The isothermal elastohydrodynamic lubrication (EHL) of a point contact was analyzed numerically by simultaneously solving the elasticity and Reynolds equations. In the elasticity analysis the contact zone was divided into equal rectangular areas, and it was assumed that a uniform pressure was applied over each area. In the numerical analysis of the Reynolds equation, a ϕ analysis (where ϕ is equal to the pressure times the film thickness to the $3/2$ power) was used to help the relaxation process. The EHL point contact analysis is applicable for the entire range of elliptical parameters and is valid for any combination of rolling and sliding within the contact.

INTRODUCTION

In many contacts between machine elements, forces are transmitted through thin, but continuous, fluid films. These fluid films as related to hydrodynamic lubrication in journal and thrust bearings have been well understood for some time, and experimental work confirms the theory. In the early 1900's, it was recognized by Martin (ref. 1) that many loaded contacts of low geometrical conformity such as gears and rolling-contact bearings probably behaved as though they were hydrodynamically lubricated. As opposed to the journal and thrust bearing counterpart, the original hydrodynamic lubrication theory of gears and rolling-contact bearings differed substantially from experimental findings. Only in recent years has the consideration of elastic deformation of contacts been coupled to hydrodynamics to yield closer agreement of theory with experiments.

Elastohydrodynamic lubrication (EHL) deals with the lubrication of elastic contacts. The analysis requires the simultaneous solution of the elasticity and Reynolds equations. The EHL theory differs from conventional hydrodynamic theory in the following ways:

*Professor of Mechanical Engineering, Leeds University, Leeds, England.

(1) In defining the film thickness in EHL theory, elastic deformation of the contact is considered.

(2) The viscosity is no longer independent of pressure, as is frequently assumed in conventional hydrodynamic theory.

Figure 1 shows the differences between the Martin (ref. 1), Hertzian, and EHL lubrication and contact conditions. Pressure and film thickness curves are shown for the respective conditions, along with a formula for minimum film thickness. The preceding definition of EHL covers not only such highly stressed lubricated machine elements as ball and roller bearings and gears, but also the performance of soft rubber seals, bearings with soft liners, and human joints. One may, therefore, classify these two types of EHL as hard EHL (ball and roller bearings and gears) and soft EHL (rubber seals, bearings with soft liners, and human joints). In this report we are concerned only with hard EHL.

When two solids are in contact under zero-load condition, one of two types of contact is experienced:

- (1) Point contact, in which the two solids touch at a single point, as in ball bearings
- (2) Line contact, in which the two solids touch along a straight or curved line, as in roller bearings

After a load is applied, the point expands to an ellipse and the line to a rectangle. Although we are concerned with loaded contacts, it is convenient to distinguish between these situations by referring to them as being either point or line contact.

Most of the work done to date in EHL has dealt with line contacts. Grubin (ref. 2) was the first to attempt a solution to the isothermal EHL line-contact problem. In Grubin's analysis it was assumed that the shape of the elastically deformed solids in a highly loaded lubricated contact was the same as the shape produced in a dry (Hertzian) contact. This assumption facilitated the solution of the Reynolds equation in the inlet region of the contact and enabled the separation of the solids in the central region of the contact to be determined with commendable accuracy.

In references 3 and 4 an empirical formula for the isothermal line-contact EHL problem was obtained. This formula shows the effect of speed, load, and material properties upon minimum film thickness and is based on their theoretical solutions. The experimental observations concur with the minimum-film-thickness formula. Forty-five years transpired from Martin's (ref. 1) rigid isothermal hydrodynamic solution until Dowson and Higginson's (refs. 3 and 4) minimum-film-thickness formula for an isothermal EHL line contact was developed.

The study of point contacts has mostly followed experimental lines. The first step toward a theoretical solution of the point-contact problem was presented by Archard and Cowking (ref. 5). They adopted an approach similar to that used by Grubin (ref. 2) for line-contact conditions. The Hertzian contact zone was assumed to form a parallel film region, and the generation of high pressure in the approaches to the Hertzian zone was

considered. Cheng (ref. 6) also used an approach similar to that used by Grubin (ref. 2) in determining a minimum film thickness for point contacts.

The reason why a complete, isothermal, point-contact EHL solution has not yet been obtained is the extreme difficulty of the numerical coupling of the elasticity and Reynolds equations. Within the last year an interesting numerical solution to the point-contact EHL problem for a sphere near a plane has been presented by Ranger (ref. 7). This solution is presented in dimensional terms, which thereby limits its general usage. A puzzling feature of Ranger's work (ref. 7) is the fact that his resulting equation for the minimum film thickness has a positive load exponent, which contradicts experiments (e. g. , ref. 8).

In the present report the theoretical foundation for the complete, isothermal, point-contact EHL problem is presented. The theory is applicable to varying values of elliptical parameters. Utilized in the theory is elasticity analysis developed by the authors in an earlier publication (ref. 9). In this analysis the contact zone was divided into equal rectangular areas, and a uniform pressure was applied over each area. The pressure-viscosity analysis of Roelands (ref. 10) is also used and is valid for any combination of rolling and sliding. Because of the length and complexity of the EHL theory, it is presented by itself. The results of the numerical analysis will appear in separate reports.

GEOMETRY OF CONTACTING ELASTIC SOLIDS

Two solids having different radii of curvature in a pair of principal planes (x and y) passing through the contact between the solids make contact at a single point under the condition of no applied load. Such a condition is called "point contact" and is shown in figure 2, where the radii of curvature are denoted by r's. In the analysis which follows, it is assumed that for convex surfaces (fig. 1) the curvature is positive but that for concave surfaces the curvature is negative. The curvature sum and difference are defined as

$$\frac{1}{R} = \frac{1}{R_x} + \frac{1}{R_y} \quad (1)$$

$$\Gamma = R \left(\frac{1}{R_x} - \frac{1}{R_y} \right) \quad (2)$$

where

$$\frac{1}{R_x} = \frac{1}{r_{Ax}} + \frac{1}{r_{Bx}} \quad (3)$$

$$\frac{1}{R_y} = \frac{1}{r_{Ay}} + \frac{1}{r_{By}} \quad (4)$$

When the two solids in figure 2 have a normal load applied to them, the result is that the point expands to an ellipse, with a being the semimajor axis and b being the semiminor axis. The normal applied load F in figure 2 lies along the axis which passes through the center of the solids at the point of contact and is perpendicular to a plane which is tangential to both solids at the point of contact. For the special case where $r_{Ay} = r_{Ax}$ and $r_{By} = r_{Bx}$, the resulting contact is a circle rather than an ellipse.

The elliptical eccentricity parameter k is defined as

$$k = \frac{a}{b} \quad (5)$$

From reference 11, k can be written in terms of the curvature difference and the elliptical integrals of the first and second kind as

$$J(k) = \sqrt{\frac{2\mathcal{F} - \mathcal{E}(1 + \Gamma)}{\mathcal{E}(1 - \Gamma)}} \quad (6)$$

where

$$\mathcal{F} = \int_0^{\pi/2} \left[1 - \left(1 - \frac{1}{k^2} \right) \sin^2 \varphi \right]^{-1/2} d\varphi \quad (7)$$

$$\mathcal{E} = \int_0^{\pi/2} \left[1 - \left(1 - \frac{1}{k^2} \right) \sin^2 \varphi \right]^{1/2} d\varphi \quad (8)$$

A one-point iteration method which has been used successfully in the past (ref. 12) is used, where

$$k_{n+1} = J(k_n) \quad (9)$$

When k is known, the semimajor and semiminor axes of the contact ellipse can be written as

$$a = \left(\frac{6k^2 \mathcal{E} RF}{\pi E'} \right)^{1/3} \quad (10)$$

$$b = \frac{a}{k} \quad (11)$$

where

$$E' = \frac{2}{\left(\frac{1 - \nu_A^2}{E_A} + \frac{1 - \nu_B^2}{E_B} \right)} \quad (12)$$

and

ν Poisson ratio

E modulus of elasticity

REYNOLDS EQUATION

The coordinate systems to be used are shown in figure 3. For the coordinate system (\tilde{X}, \tilde{Y}) the general Reynolds equations for EHL of point contacts from reference 13 gives the following:

$$\frac{\partial}{\partial \tilde{X}} \left(\frac{\rho h^3}{12\eta} \frac{\partial \rho}{\partial \tilde{X}} \right) + \frac{\partial}{\partial \tilde{Y}} \left(\frac{\rho h^3}{12\eta} \frac{\partial \rho}{\partial \tilde{Y}} \right) = \frac{\partial}{\partial \tilde{X}} \left[\rho h \frac{(u_A + u_B)}{2} \right] + \frac{\partial}{\partial \tilde{Y}} \left[\rho h \frac{(v_A + v_B)}{2} \right] \quad (13)$$

where

u_A surface velocity of solid A in \tilde{X} direction

u_B surface velocity of solid B in \tilde{X} direction

v_A surface velocity of solid A in \tilde{Y} direction

v_B surface velocity of solid B in \tilde{Y} direction

The surface velocities are assumed to be constant and, therefore, equation (13) can be rewritten as

$$\frac{\partial}{\partial \tilde{X}} \left(\frac{\rho h^3}{\eta} \frac{\partial p}{\partial \tilde{X}} \right) + \frac{\partial}{\partial \tilde{Y}} \left(\frac{\rho h^3}{\eta} \frac{\partial p}{\partial \tilde{Y}} \right) = 12 \left[u \frac{\partial(\rho h)}{\partial \tilde{X}} + v \frac{\partial(\rho h)}{\partial \tilde{Y}} \right] \quad (14)$$

where

$$u = \frac{u_A + u_B}{2} \quad (15)$$

$$v = \frac{v_A + v_B}{2} \quad (16)$$

By introducing V and θ , where

$$V = \sqrt{u^2 + v^2} \quad (17)$$

$$\theta = \tan^{-1} \left(\frac{v}{u} \right) \quad (18)$$

equation (14) becomes

$$\frac{\partial}{\partial \tilde{X}} \left(\frac{\rho h^3}{\eta} \frac{\partial p}{\partial \tilde{X}} \right) + \frac{\partial}{\partial \tilde{Y}} \left(\frac{\rho h^3}{\eta} \frac{\partial p}{\partial \tilde{Y}} \right) = 12V \left[\cos \theta \frac{\partial(\rho h)}{\partial \tilde{X}} + \sin \theta \frac{\partial(\rho h)}{\partial \tilde{Y}} \right] \quad (19)$$

By letting

$$\left. \begin{aligned} X &= \frac{\tilde{X}}{b} & \bar{\eta} &= \frac{\eta}{\eta_0} \\ Y &= \frac{\tilde{Y}}{a} & H &= \frac{h}{R} \\ \bar{\rho} &= \frac{\rho}{\rho_0} & P &= \frac{p}{E'} \end{aligned} \right\} \quad (20)$$

equation (19) can be written as

$$\boxed{\frac{\partial}{\partial X} \left(\frac{\bar{\rho} H^3}{\bar{\eta}} \frac{\partial P}{\partial X} \right) + \frac{1}{k^2} \frac{\partial}{\partial Y} \left(\frac{\bar{\rho} H^3}{\bar{\eta}} \frac{\partial P}{\partial Y} \right) = 12U \left(\frac{b}{R} \right) \left[\cos \theta \frac{\partial(\bar{\rho} H)}{\partial X} + \frac{\sin \theta}{k} \frac{\partial(\bar{\rho} H)}{\partial Y} \right]} \quad (21)$$

where

$$U = \frac{V\eta_0}{RE'} \quad (22)$$

Equation (21) is the Reynolds equation for which the dimensionless pressure P will be determined. However, before proceeding, the dimensionless density $\bar{\rho}$, the dimensionless viscosity $\bar{\eta}$, and the dimensionless film thickness H need to be expressed.

Density

From reference 14 the dimensionless density for mineral oil can be written as

$$\bar{\rho} = 1 + \frac{0.009 p}{1 + 0.026 p}$$

where

p gage pressure, ton/in.²

Therefore, the general expression for the dimensionless density can be written as

$$\boxed{\bar{\rho} = 1 + \frac{\alpha PE'}{1 + \beta PE'}} \quad (23)$$

where

α, β constants dependent on fluid

Viscosity

Roelands (ref. 10) has undertaken a wide-ranging study of the effect of pressure upon the viscosity of lubricants. For isothermal conditions, his equation (p. 95, ref. 10) can be written as

$$\log \eta + 1.200 = (\log \eta_0 + 1.200) \left(1 + \frac{p}{2000}\right)^z \quad (24)$$

where

- p gage pressure, kgf/cm²
 η_0 atmospheric viscosity
 z viscosity pressure index, a dimensionless constant

Rearranging terms gives

$$\boxed{\bar{\eta} = \left(\frac{\eta_\infty}{\eta_0} \right) \left[1 - \left(1 + \frac{PE'}{\gamma} \right)^z \right]} \quad (25)$$

where

- η_∞ 0.00631 N-sec/m² (0.0631 cP)
 γ constant equal to 19 609 N/cm² (28 440 lb/in.²)

In equations (23) and (25), care must be taken to ensure that the same dimensions are used in defining the constants.

Film Thickness

A simplified expression for defining the film thickness may be written as

$$h(\tilde{X}, \tilde{Y}) = h_0 + S(\tilde{X}, \tilde{Y}) + w(\tilde{X}, \tilde{Y}) \quad (26)$$

where

- h_0 central film thickness
 $S(\tilde{X}, \tilde{Y})$ separation due to geometry of ellipsoidal solids
 $w(\tilde{X}, \tilde{Y})$ elastic deformation

The separation due to the geometry of the two ellipsoidal solids shown in figure 2 can be adequately described by an equivalent ellipsoidal solid near a plane. The geometrical requirement is that the separation of the ellipsoidal solids in the initial and equivalent situations should be the same at equal values of \tilde{X} . Therefore, from figure 3 the separation due to the geometry of the two ellipsoids shown in figure 2 can be written for an ellipsoidal solid near a plane as

$$s(\tilde{X}, \tilde{Y}) = \frac{(\tilde{X} - mb)^2}{2R_x} + \frac{(\tilde{Y} - la)^2}{2R_y} \quad (27)$$

where

m constant used to determine length of inlet region

l constant used to determine length of side leakage region

For purposes of illustration we will continue to use the mesh described in figure 3, where $m = 4$ and $l = 2$. However, the equations developed will be written in general terms.

Figure 4 gives a physical description of the film thickness and its components for an ellipsoidal solid near a plane. Here it is assumed that $y = 0$, or $\tilde{Y} = la$, in figure 3.

Substituting equation (27) into equation (26) while at the same time making this equation dimensionless gives

$$\boxed{H(X, Y) = H_0 + \frac{b^2(X - m)^2}{2RR_x} + \frac{a^2(Y - l)^2}{2RR_y} + \frac{w(X, Y)}{R}} \quad (28)$$

where

$$H = \frac{h}{R}$$

In reference 9 the elastic deformation (w in eq. (28)) of an equivalent ellipsoidal solid near a plane in contact and subjected to a Hertzian stress distribution has been evaluated numerically. In the analysis of reference 9 the contact zone was divided into equal rectangular areas, and it was assumed that a uniform pressure was applied over each area. The results of reference 9 indicate that the division of the semimajor and semiminor axes into five equal subdivisions is sufficient to obtain the elastic deformation with adequate accuracy. Making use of the results of reference 9, figure 3 shows an example of dividing the area in and around the contact zone into equal rectangular areas. In figure 3 the outlet region of the contact is not extended as much as the inlet region since previous investigators (e. g., ref. 15) have found the pressure gradients at the outlet to be very large, with the pressure quickly setting to zero.

Therefore, by using figure 3 and the results of reference 9, the elastic deformation can be written as

$$w_{\bar{k}, \bar{l}}(X, Y) = \frac{2}{\pi} \sum_{j=1, 2, \dots}^{2l \times c} \sum_{i=1, 2, \dots}^{(m+n) \times d} P_{i, j} D_{\bar{m}, \bar{n}} \quad (29)$$

where

n constant used to determine length of outlet region

c number of equal divisions in semimajor axis

d number of equal divisions in semiminor axis

$$\bar{m} = |\bar{k} - i| + 1$$

$$\bar{n} = |\bar{l} - j| + 1$$

$$\begin{aligned} D = b \left(X + \frac{1}{2d} \right) \ln & \left[\frac{k \left(Y + \frac{1}{2c} \right) + \sqrt{k^2 \left(Y + \frac{1}{2c} \right)^2 + \left(X + \frac{1}{2d} \right)^2}}{k \left(Y - \frac{1}{2c} \right) + \sqrt{k^2 \left(Y - \frac{1}{2c} \right)^2 + \left(X + \frac{1}{2d} \right)^2}} \right] \\ & + a \left(Y + \frac{1}{2c} \right) \ln \left[\frac{\left(X + \frac{1}{2d} \right) + \sqrt{k^2 \left(Y + \frac{1}{2c} \right)^2 + \left(X + \frac{1}{2d} \right)^2}}{\left(X - \frac{1}{2d} \right) + \sqrt{k^2 \left(Y + \frac{1}{2c} \right)^2 + \left(X - \frac{1}{2d} \right)^2}} \right] \\ & + b \left(X - \frac{1}{2d} \right) \ln \left[\frac{k \left(Y - \frac{1}{2c} \right) + \sqrt{k^2 \left(Y - \frac{1}{2c} \right)^2 + \left(X - \frac{1}{2d} \right)^2}}{k \left(Y + \frac{1}{2c} \right) + \sqrt{k^2 \left(Y + \frac{1}{2c} \right)^2 + \left(X - \frac{1}{2d} \right)^2}} \right] \\ & + a \left(Y - \frac{1}{2c} \right) \ln \left[\frac{\left(X - \frac{1}{2d} \right) + \sqrt{k^2 \left(Y - \frac{1}{2c} \right)^2 + \left(X - \frac{1}{2d} \right)^2}}{\left(X + \frac{1}{2d} \right) + \sqrt{k^2 \left(Y - \frac{1}{2c} \right)^2 + \left(X + \frac{1}{2d} \right)^2}} \right] \end{aligned} \quad (30)$$

(In fig. 3, $c = d = 5$.) Equation (31) points out more explicitly the meaning of equation (29) while making use of figure 3. The elastic deformation at the center of the rectangular area $w_{9, 5}$ (fig. 3) caused by the pressure on the various rectangular areas in and around the contact ellipse can be written as

$$w_{9,5} = \frac{2}{\pi} \begin{bmatrix} P_{1,1} D_{9,5} + P_{2,1} D_{8,5} + \dots + P_{35,1} D_{27,5} \\ + P_{1,2} D_{9,4} + P_{2,2} D_{8,4} + \dots + P_{35,2} D_{27,4} \\ \vdots \\ + P_{1,20} D_{9,16} + P_{2,20} D_{8,16} + \dots + P_{35,20} D_{27,16} \end{bmatrix} \quad (31)$$

PHI (ϕ) SOLUTION

Having defined the density, viscosity, and film thickness we can return to the problem of solving the Reynolds equation. It is well known (e.g., ref. 16) that the dimensionless pressure P of the Reynolds equation plotted as a function of X exhibits a very localized pressure field, giving high values of $\partial P / \partial X$ and $\partial^2 P / \partial X^2$. Such a condition with high gradients is not welcomed when performing a numerical analysis by means of relaxation methods. In order to produce a much gentler curve, a parameter ϕ is introduced, where

$$\phi = PH^{3/2} \quad (32)$$

The pressure P is small at large values of film thickness H and conversely. This substitution also has the advantage of eliminating all terms containing derivatives of products of H and P or H and ϕ . Therefore, by using equation (32), equation (21) can be written as

$$\begin{aligned} \frac{\partial}{\partial X} \left[\frac{\bar{\rho}}{\eta} \left(H^{3/2} \frac{\partial \phi}{\partial X} - \frac{3}{2} \phi H^{1/2} \frac{\partial H}{\partial X} \right) \right] + \frac{1}{k^2} \frac{\partial}{\partial Y} \left[\frac{\bar{\rho}}{\eta} \left(H^{3/2} \frac{\partial \phi}{\partial Y} - \frac{3}{2} \phi H^{1/2} \frac{\partial H}{\partial Y} \right) \right] \\ = 12U \left(\frac{b}{R} \right) \left[\cos \theta \frac{\partial (\bar{\rho} H)}{\partial X} + \frac{\sin \theta}{k} \frac{\partial (\bar{\rho} H)}{\partial Y} \right] \end{aligned}$$

Expanding this equation yields

$$\begin{aligned} H^{3/2} \left[\frac{\partial}{\partial X} \left(\frac{\bar{\rho}}{\eta} \frac{\partial \phi}{\partial X} \right) + \frac{1}{k^2} \frac{\partial}{\partial Y} \left(\frac{\bar{\rho}}{\eta} \frac{\partial \phi}{\partial Y} \right) \right] - \frac{3\phi}{2} \left[\frac{\partial}{\partial X} \left(\frac{\bar{\rho}}{\eta} H^{1/2} \frac{\partial H}{\partial X} \right) + \frac{1}{k^2} \frac{\partial}{\partial Y} \left(\frac{\bar{\rho}}{\eta} H^{1/2} \frac{\partial H}{\partial Y} \right) \right] \\ = 12U \left(\frac{b}{R} \right) \left[\cos \theta \frac{\partial (\bar{\rho} H)}{\partial X} + \frac{\sin \theta}{k} \frac{\partial (\bar{\rho} H)}{\partial Y} \right] \end{aligned} \quad (33)$$

Finite Difference Representation

The finite difference method will be used to develop the various terms in equation (33). Figure 5 shows the mesh to be used as related to the dimensionless coordinates X and Y . Equation (33) must be written for the point (i, j) in figure 5 by substituting for the derivatives expressions that involve values of ϕ , H , $\bar{\rho}$, and $\bar{\eta}$ at the surrounding points.

At the three points $X_{i-1, j}$, $X_{i, j}$, and $X_{i+1, j}$, a function of X such as ψ can be represented by a parabola, where

$$\psi = AX^2 + BX + C \quad (34)$$

The parabola and corresponding points are shown in figure 6. The expressions for $\psi_{i-1, j}$, $\psi_{i, j}$, and $\psi_{i+1, j}$ can be written directly from equation (34) as

$$\psi_{i-1, j} = AX_{i-1, j}^2 + BX_{i-1, j} + C \quad (35)$$

$$\psi_{i, j} = AX_{i, j}^2 + BX_{i, j} + C \quad (36)$$

$$\psi_{i+1, j} = AX_{i+1, j}^2 + BX_{i+1, j} + C \quad (37)$$

From figure 6 the following equations can be written:

$$X_{i, j} = X_{i-1, j} + \frac{1}{d}$$

$$X_{i+1, j} = X_{i-1, j} + \frac{2}{d}$$

Substituting these expressions into equations (36) and (37) gives

$$\psi_{i, j} = A\left(X_{i-1, j} + \frac{1}{d}\right)^2 + B\left(X_{i-1, j} + \frac{1}{d}\right) + C \quad (38)$$

$$\psi_{i+1, j} = A\left(X_{i-1, j} + \frac{2}{d}\right)^2 + B\left(X_{i-1, j} + \frac{2}{d}\right) + C \quad (39)$$

Therefore, given equations (35), (38), and (39), it is possible to solve for A , B , and C to give

$$A = 0.5 \, d^2(\psi_{i+1,j} - 2\psi_{i,j} + \psi_{i-1,j}) \quad (40)$$

$$B = 0.5 \, d(4\psi_{i,j} - 3\psi_{i-1,j} - \psi_{i+1,j}) - 2AX_{i-1,j} \quad (41)$$

$$C = \psi_{i-1,j} - BX_{i-1,j} - AX_{i-1,j}^2 \quad (42)$$

The following derivatives can be written by using equations (40) to (42):

$$\frac{\partial \psi_{i-1,j}}{\partial X_{i-1,j}} = 2AX_{i-1,j} + B = B' = 0.5 \, d(4\psi_{i,j} - 3\psi_{i-1,j} - \psi_{i+1,j}) \quad (43)$$

$$\frac{\partial \psi_{i,j}}{\partial X_{i,j}} = 2AX_{i,j} + B = 2A\left(X_{i-1,j} + \frac{1}{d}\right) + B = 2AX_{i-1,j} + B + \frac{2A}{d} = B' + \frac{2A}{d}$$

$$\frac{\partial \psi_{i,j}}{\partial X_{i,j}} = 0.5 \, d(\psi_{i+1,j} - \psi_{i-1,j}) \quad (44)$$

$$\frac{\partial \psi_{i+1,j}}{\partial X_{i+1,j}} = 2AX_{i+1,j} + B = 2A\left(X_{i-1,j} + \frac{2}{d}\right) + B = 0.5 \, d(3\psi_{i+1,j} - 4\psi_{i,j} + \psi_{i-1,j}) \quad (45)$$

$$\frac{\partial^2 \psi_{i-1,j}}{\partial X_{i-1,j}^2} = \frac{\partial^2 \psi_{i,j}}{\partial X_{i,j}^2} = \frac{\partial^2 \psi_{i+1,j}}{\partial X_{i+1,j}^2} = 2A = d^2(\psi_{i+1,j} - 2\psi_{i,j} + \psi_{i-1,j}) \quad (46)$$

Having developed these basic equations with the dummy variable ψ , we can now proceed to develop the various terms in equation (33) by using the finite difference format developed in this section. The following equation is written for the point (i, j):

$$\frac{\partial}{\partial X} \left(\frac{\bar{\rho}}{\eta} H^{1/2} \frac{\partial H}{\partial X} \right) = 0.5 \, d \left[\frac{\bar{\rho}_{i+1,j}}{\eta_{i+1,j}} \sqrt{H_{i+1,j}} \left(\frac{\partial H}{\partial X} \right)_{i+1,j} - \frac{\bar{\rho}_{i-1,j}}{\eta_{i-1,j}} \sqrt{H_{i-1,j}} \left(\frac{\partial H}{\partial X} \right)_{i-1,j} \right] \quad (47)$$

By using equations (42) and (44) the following equations can be written:

$$\left(\frac{\partial H}{\partial X} \right)_{i+1,j} = 0.5 \, d(3H_{i+1,j} - 4H_{i,j} + H_{i-1,j}) \quad (48)$$

$$\left(\frac{\partial H}{\partial X}\right)_{i-1,j} = 0.5 d(-H_{i+1,j} + 4H_{i,j} - 3H_{i-1,j}) \quad (49)$$

Substituting equations (48) and (49) into (47) gives

$$\begin{aligned} \frac{\partial}{\partial X} \left(\frac{\bar{\rho}}{\bar{\eta}} H^{1/2} \frac{\partial H}{\partial X} \right) = 0.25 d^2 \left[\frac{\bar{\rho}_{i+1,j}}{\bar{\eta}_{i+1,j}} \sqrt{H_{i+1,j}} (3H_{i+1,j} - 4H_{i,j} + H_{i-1,j}) \right. \\ \left. + \frac{\bar{\rho}_{i-1,j}}{\bar{\eta}_{i-1,j}} \sqrt{H_{i-1,j}} (H_{i+1,j} - 4H_{i,j} + 3H_{i-1,j}) \right] \end{aligned} \quad (50)$$

Thus, the following equation can be directly written:

$$\frac{\partial}{\partial X} \left(\frac{\bar{\rho}}{\bar{\eta}} \frac{\partial \phi}{\partial X} \right) = 0.25 d^2 \left[\frac{\bar{\rho}_{i+1,j}}{\bar{\eta}_{i+1,j}} (3\phi_{i+1,j} - 4\phi_{i,j} + \phi_{i-1,j}) + \frac{\bar{\rho}_{i-1,j}}{\bar{\eta}_{i-1,j}} (\phi_{i+1,j} - 4\phi_{i,j} + 3\phi_{i-1,j}) \right] \quad (51)$$

$$\frac{\partial}{\partial X} (\bar{\rho}H) = 0.5 d(\bar{\rho}_{i+1,j}H_{i+1,j} - \bar{\rho}_{i-1,j}H_{i-1,j}) \quad (52)$$

The derivatives with respect to Y can be obtained directly by substituting c for d, the subscript i, j-1 for i-1, j, and the subscript i, j+1 for i+1, j.

$$\begin{aligned} \frac{\partial}{\partial Y} \left(\frac{\bar{\rho}}{\bar{\eta}} H^{1/2} \frac{\partial H}{\partial Y} \right) = 0.25 c^2 \left[\frac{\bar{\rho}_{i,j+1}}{\bar{\eta}_{i,j+1}} \sqrt{H_{i,j+1}} (3H_{i,j+1} - 4H_{i,j} + H_{i,j-1}) \right. \\ \left. + \frac{\bar{\rho}_{i,j-1}}{\bar{\eta}_{i,j-1}} \sqrt{H_{i,j-1}} (H_{i,j+1} - 4H_{i,j} + 3H_{i,j-1}) \right] \end{aligned} \quad (53)$$

$$\frac{\partial}{\partial Y} \left(\frac{\bar{\rho}}{\bar{\eta}} \frac{\partial \phi}{\partial Y} \right) = 0.25 c^2 \left[\frac{\bar{\rho}_{i,j+1}}{\bar{\eta}_{i,j+1}} (3\phi_{i,j+1} - 4\phi_{i,j} + \phi_{i,j-1}) + \frac{\bar{\rho}_{i,j-1}}{\bar{\eta}_{i,j-1}} (\phi_{i,j+1} - 4\phi_{i,j} + 3\phi_{i,j-1}) \right] \quad (54)$$

$$\frac{\partial}{\partial Y} (\bar{\rho}H) = 0.5 c(\bar{\rho}_{i,j+1}H_{i,j+1} - \bar{\rho}_{i,j-1}H_{i,j-1}) \quad (55)$$

Substituting equations (50) to (55) into equation (33) while collecting terms gives

$$\overline{A}_{i,j}\phi_{i+1,j} + \overline{B}_{i,j}\phi_{i,j-1} + \overline{C}_{i,j}\phi_{i-1,j} + \overline{D}_{i,j}\phi_{i,j+1} - \overline{L}_{i,j}\phi_{i,j} - \overline{M}_{i,j} = 0 \quad (56)$$

where

$$\mu = \frac{\bar{\rho}}{\eta} \quad (57)$$

$$\overline{A}_{i,j} = 3\mu_{i+1,j} + \mu_{i-1,j} \quad (58)$$

$$\overline{B}_{i,j} = \left(\frac{c}{dk}\right)^2 (\mu_{i,j+1} + 3\mu_{i,j-1}) \quad (59)$$

$$\overline{C}_{i,j} = \mu_{i+1,j} + 3\mu_{i-1,j} \quad (60)$$

$$\overline{D}_{i,j} = \left(\frac{c}{dk}\right)^2 (3\mu_{i,j+1} + \mu_{i,j-1}) \quad (61)$$

$$\begin{aligned} \overline{L}_{i,j} = & 4(\mu_{i+1,j} + \mu_{i-1,j}) + 4\left(\frac{c}{dk}\right)^2 (\mu_{i,j+1} + \mu_{i,j-1}) \\ & + \frac{3}{2H_{i,j}^{3/2}} \left\{ \mu_{i+1,j} \sqrt{H_{i+1,j}} (3H_{i+1,j} - 4H_{i,j} + H_{i-1,j}) + \mu_{i-1,j} \sqrt{H_{i-1,j}} (H_{i+1,j} - 4H_{i,j} + 3H_{i-1,j}) + \left(\frac{c}{dk}\right)^2 \right. \\ & \times \left[\mu_{i,j+1} \sqrt{H_{i,j+1}} (3H_{i,j+1} - 4H_{i,j} + H_{i,j-1}) + \mu_{i,j-1} \sqrt{H_{i,j-1}} (H_{i,j+1} - 4H_{i,j} + 3H_{i,j-1}) \right] \Big\} \end{aligned} \quad (62)$$

$$\overline{M}_{i,j} = \frac{24Ub}{dRH_{i,j}^{3/2}} \left[\cos \theta (\bar{\rho}_{i+1,j} H_{i+1,j} - \bar{\rho}_{i-1,j} H_{i-1,j}) + \frac{c \sin \theta}{dk} (\bar{\rho}_{i,j+1} H_{i,j+1} - \bar{\rho}_{i,j-1} H_{i,j-1}) \right] \quad (63)$$

Boundary Conditions

The boundary conditions are the following:

(1) At the edges of the rectangular computation zone (fig. 3) the pressure will be zero, therefore implying that ϕ is also zero. Specifically, this means that along the bottom of figure 3, $\phi_{i,1} = 0$; along the left side, $\phi_{i,j} = 0$; along the top, $\phi_{i,20} = 0$; and along the right side, $\phi_{35,j} = 0$.

(2) At the cavitation boundary, $P = 0$ for

$$\frac{\partial P}{\partial X} = \frac{\partial P}{\partial Y} = 0$$

This condition is commonly known as the Reynolds condition and will be satisfied by simply resetting $\phi_{i,j}$ to zero whenever it occurs as a negative value.

(3) The term $\phi_{i,j}$ is not allowed to exceed ϕ_{\max} , where $\phi_{\max} = \delta\phi_H$ (where ϕ_H is equal to ϕ when ϕ is evaluated at the center of a Hertzian contact).

Initial Conditions

Outside the Hertzian contact ellipse the pressure is initially assumed to be zero, and therefore $\phi = 0$ there. That is, if $P = 0$,

$$\phi = 0$$

when

$$(X - m)^2 + (Y - l)^2 \geq 1$$

Inside the Hertzian contact ellipse the pressure is initially assumed to be Hertzian; that is,

$$P = \frac{3F}{2\pi abE'} \sqrt{1 - (X - m)^2 - (Y - l)^2} \quad (64)$$

or

$$\phi = \frac{3FH^{3/2}}{2\pi abE'} \sqrt{1 - (X - m)^2 - (Y - l)^2} \quad (65)$$

when

$$(X - m)^2 + (Y - l)^2 < 1$$

Relaxation Method

If subscript n is the iterant and $\phi_{i,j}$ is the particular solution to be found, the relaxation method known as the Gauss-Seidel method can be expressed as

$$\phi_{i,j,n+1} = \phi_{i,j,n} - \lambda \left(\frac{\overline{M}_{i,j} - \overline{A}_{i,j}\phi_{i+1,j,n} - \overline{B}_{i,j}\phi_{i,j-1,n+1} - \overline{C}_{i,j}\phi_{i-1,j,n+1} - \overline{D}_{i,j}\phi_{i,j+1,n}}{\overline{L}_{i,j}} + \phi_{i,j,n} \right) \quad (66)$$

where λ is an overrelaxation factor which is initially set to 1.4. Therefore, equation (66) is used starting with node (2,2) then continuing with (3,2), . . . , until (M,2); followed by (2,3), (3,3), . . . , (M,3); and ending with (2,N), (3,N), . . . , (M,N), where

$$M = (n + m)d - 1$$

$$N = 2lc - 1$$

The relaxation procedure described by equation (66) is continued until

$$\sum_{j=2,3,\dots}^N \sum_{i=2,3,\dots}^M \frac{|\phi_{i,j,n+1} - \phi_{i,j,n}|}{\phi_{i,j,n+1}} < \xi_1$$

where $\xi_1 = 0.1$, initially.

Dimensionless Pressure Loop

The relaxation method provides values of $\phi_{i,j}$ for every point within the mesh. Having determined $\phi_{i,j}$, we can write the dimensionless pressure as

$$P_{i,j} = \phi_{i,j}(H_{i,j})^{-3/2} \quad (67)$$

With these new values of the dimensionless pressure, new values of the dimensionless viscosity, density, and film thickness can be evaluated. Thus, the coefficients of equation (66) ($\overline{A}_{i,j}$, $\overline{B}_{i,j}$, . . . , $\overline{L}_{i,j}$) should also change. Accordingly, it is necessary to reenter the relaxation loop. This process is continued until the following inequality is satisfied:

$$\sum_{j=2,3,\dots}^N \sum_{i=2,3,\dots}^M \frac{|P_{i,j,n+1} - P_{i,j,n}|}{P_{i,j,n+1}} < \xi$$

NORMAL APPLIED LOAD

The central dimensionless film thickness H_0 was initially estimated. The next task is then to find the correct value for H_0 . In order to do this, the integrated normal applied load must be evaluated, where

$$\overline{F} = E'ab \int_0^{m+n} \int_0^{2l} P \, dY \, dX \quad (68)$$

By applying Simpson's rule, this double integral can be rewritten as

$$\overline{F} = \frac{4E'ab}{9cd} \left[\begin{array}{l} 2(2P_{2,2} + P_{2,3} + 2P_{2,4} + P_{2,5} + \dots + 2P_{2,2l-2} + P_{2,2l-1}) \\ + (2P_{3,2} + P_{3,3} + 2P_{3,4} + P_{3,5} + \dots + 2P_{3,2l-2} + P_{3,2l-1}) \\ \vdots \\ + 2(2P_{m+n-2,2} + P_{m+n-2,3} + 2P_{m+n-2,4} + P_{m+n-2,5} + \dots + 2P_{m+n-2,2l-2} + P_{m+n-2,2l-1}) \\ + (2P_{m+n-1,2} + P_{m+n-1,3} + 2P_{m+n-1,4} + P_{m+n-1,5} + \dots + 2P_{m+n-1,2l-2} + P_{m+n-1,2l-1}) \end{array} \right]$$

This equation can be rewritten simply as

$$\overline{F} = \frac{4E'ab}{9cd} \sum_{i=2,3,\dots}^{m+n-1} 2^{q_i} \left(\sum_{j=2,3,\dots}^{2l-1} 2^{q_{2P_{i,j}}} \right) \quad (69)$$

where

$$\begin{aligned} q_1 &= 0 & \text{if } i \text{ is odd} \\ q_1 &= 1 & \text{if } i \text{ is even} \end{aligned}$$

$$q_2 = 0 \quad \text{if } j \text{ is odd}$$

$$q_2 = 1 \quad \text{if } j \text{ is even}$$

By using the trapezoidal rule, the normal applied load can also be expressed as

$$\overline{F} = \frac{E'ab}{cd} \sum_{i=2,3,\dots}^{m+n-1} \sum_{j=2,3,\dots}^{2l-1} P_{ij} \quad (70)$$

Both equations (69) and (70) will be programmed to serve as a check on one another.

When the dimensionless film thickness is evaluated from equation (28), the smallest value of H , called H_{\min} , is retained as well as the location of H_{\min} . The location of H_{\min} is designated by $X = X^*$ and $Y = Y^*$. The current values of the integrated normal applied load \overline{F} , the initially specified normal applied load F , the minimum film thickness H_{\min} , as well as the location of the minimum film thickness (X^*, Y^*), are used to make a new estimate for the central film thickness \overline{H}_O , which can be expressed as

$$\overline{H}_O = H_{\min} \left(\frac{\overline{F}}{F} \right)^\Lambda - \frac{b^2(X^* - m)^2}{2RR_x} - \frac{a^2(Y^* - l)^2}{2RR_y} - \frac{w(X^*, Y^*)}{R} \quad (71)$$

where Λ is a constant, initially set at 0.5.

With the new value of the dimensionless central film thickness, the film thickness must be recalculated and reentry into the relaxation and pressure loop is required. This process is continued until the following inequality is satisfied:

$$\frac{|\overline{H}_O - H_O|}{\overline{H}_O} < \xi_3$$

where ξ_3 is 0.0005 initially.

FLOW RATE

The mass flow rate in the \tilde{X} and \tilde{Y} directions shown in figure 3 can be written as

$$q_{\tilde{X}} = u\rho h - \frac{\rho h^3}{12\eta} \frac{\partial p}{\partial \tilde{X}}$$

$$q_{\tilde{Y}} = v\rho h - \frac{\rho h^3}{12\eta} \frac{\partial p}{\partial \tilde{Y}}$$

By making use of equation (20), the preceding equations can be made dimensionless:

$$Q_X = \frac{q_{\tilde{X}}\eta_0}{\rho_0 E' R^2} = \left(\frac{u\eta_0}{RE'} \right) \bar{\rho} H - \frac{\bar{\rho} R H^3}{12b\bar{\eta}} \frac{\partial P}{\partial X}$$

$$Q_Y = \frac{q_{\tilde{Y}}\eta_0}{\rho_0 E' R^2} = \left(\frac{v\eta_0}{RE'} \right) \bar{\rho} H - \frac{\bar{\rho} R H^3}{12a\bar{\eta}} \frac{\partial P}{\partial Y}$$

By letting $u = V \cos \theta$, $v = V \sin \theta$ and $U = V\eta_0/E'R$, these equations can be rewritten as

$$Q_X = U\bar{\rho} H \cos \theta - \frac{\bar{\rho} H^3}{12\bar{\eta}} \left(\frac{R}{b} \right) \frac{\partial P}{\partial X} \quad (72)$$

$$Q_Y = U\bar{\rho} H \sin \theta - \frac{\bar{\rho} H^3}{12\bar{\eta}} \left(\frac{R}{a} \right) \frac{\partial P}{\partial Y} \quad (73)$$

$$Q = \sqrt{Q_X^2 + Q_Y^2} \quad (74)$$

$$\varphi = \tan^{-1} \left(\frac{Q_Y}{Q_X} \right) \quad (75)$$

where

$$\frac{\partial P}{\partial X} = \frac{d}{2} (P_{i+1,j} - P_{i-1,j}) \quad (76)$$

$$\frac{\partial P}{\partial Y} = \frac{c}{2} (P_{i,j+1} - P_{i,j-1}) \quad (77)$$

FLOW CHARTS

Figures 7 and 8 are flow charts for the numerical solution on the digital computer of the equations developed in the analysis. Figure 7 is the flow chart of the main program. There are essentially three loops within the main program: In the relaxation loop, $\phi_{i,j,n+1}$ is generated. In the pressure loop, the new values of $\phi_{i,j,n+1}$ of the relaxation loop result in new values of pressure $P_{i,j,n+1}$ which in turn result in new values of film thickness $H_{i,j}$, new values of viscosity $\bar{\eta}_{i,j}$, and new values of density $\bar{\rho}_{i,j}$. The final loop is the central film thickness loop H_0 which ensures that the integrated normal applied load agrees with the initially specified value.

Figure 8 shows the flow chart of the subroutine SUB6. Here it can be seen that a number of calculations occur only once and need not be repeated on reentry to this subroutine. With a new pressure distribution the elastic deformation is recalculated and leaves this subroutine with a new film thickness and, therefore, a new $\phi_{i,j,n}$.

CONCLUDING REMARKS

A procedure for the numerical solution of the complete, isothermal, elastohydrodynamic lubrication problem for point contacts is outlined. This procedure calls for the simultaneous solution of the elasticity and Reynolds equations. In the elasticity analysis the contact zone was divided into equal rectangular areas. It was assumed that a uniform pressure was applied over each area. In the numerical analysis of the Reynolds equation the parameter $\phi = PH^{3/2}$, where P is dimensionless pressure and H is dimensionless film thickness, was introduced in order to help the relaxation process.

The analysis is applicable to the complete range of elliptical parameters and is valid for any combination of rolling and sliding within a point contact.

Lewis Research Center,
National Aeronautics and Space Administration,
Cleveland, Ohio, May 28, 1975,
505-04.

APPENDIX - SYMBOLS

A, B, C	constants defined in eq. (34)
$\overline{A}, \overline{B}, \overline{C}, \overline{D}, \overline{L}, \overline{M}$	relaxation coefficients
a	semimajor axis of contact ellipse
\overline{a}	$a/2c$
b	semiminor axis of contact ellipse
\overline{b}	$b/2d$
c	number of equal divisions of semimajor axis
D	defined by eq. (30)
d	number of equal divisions of semiminor axis
E	modulus of elasticity
E'	$\frac{2}{\left(\frac{1 - \nu_A^2}{E_A} + \frac{1 - \nu_B^2}{E_B} \right)}$
\mathcal{E}	elliptical integral of second kind
F	normal applied load
\overline{F}	integrated normal applied load
\mathcal{F}	elliptical integral of first kind
G	dimensionless material parameter
H	dimensionless film thickness, h/R
H_{\min}	dimensionless minimum film thickness, h_{\min}/R
H_0	dimensionless central film thickness, h_0/R
h	film thickness
h_{\min}	minimum film thickness
h_0	central film thickness
J	function of k (eq. (9))
k	elliptical eccentricity parameter, a/b
P	dimensionless pressure, p/E'

p	pressure
Q	dimensionless mass flow rate, $\rho\eta_0/\rho_0 E'R^2$
q	mass flow rate
R	effective radius
r	radius of curvature
U	dimensionless speed parameter, $V\eta_0/RE'$
u	surface velocity in \tilde{X} direction
V	$\sqrt{u^2 + v^2}$
v	surface velocity in \tilde{Y} direction
W	dimensionless load parameter, $F/E'R_x R_y$
w	total elastic deformation
w'	total elastic deformation at center of contact
x, X, \tilde{X} y, Y, \tilde{Y}	coordinate systems defined in report
z	viscosity pressure index, a dimensionless constant
α, β	constants defining fluid used (eq. (23))
Γ	curvature difference
η	lubricant viscosity
$\bar{\eta}$	dimensionless viscosity, η/η_0
η_0	atmospheric viscosity
θ	angle of resultant velocity vectors (eq. (18))
λ	overrelaxation factor
μ	$\bar{\rho}/\bar{\eta}$
ν	Poisson ratio
ρ	lubricant density
$\bar{\rho}$	dimensionless density, ρ/ρ_0
φ	defined by eq. (75)
ϕ	$PH^{3/2}$

Subscripts:


A **solid A**

B **solid B**

x, y **coordinate system defined in report**

REFERENCES

1. Martin, H. M.: The Lubrication of Gear-Teeth. Engineering (London), vol. 102, 1916, pp. 119-121.
2. Grubin, A. N.; and Vinogradova, I. E., eds.: Investigation of the Contact of Machine Components. Central Scientific Research Institute for Technology and Mechanical Engineering, Book 30, (D. S. I. R. translation 337), Moscow, 1949.
3. Dowson, D.; and Higginson, G. R.: A Numerical Solution to the Elastohydrodynamic Problem. J. Mech. Eng. Sci., vol. 1, no. 1, 1959, pp. 6-15.
4. Dowson, D.; and Higginson, G. R.: New Roller-Bearing Lubrication Formula. Engineering (London), vol. 192, no. 4972, Aug. 1961, pp. 158-159.
5. Archard, J. F.; and Cowking, E. W.: Elastohydrodynamic Lubrication of Point Contacts. Proc. Instru. Mech. Engrs., vol. 180, pt. 3B, 1965-1966, pp. 47-56.
6. Cheng, H. S.: A Numerical Solution of the Elastohydrodynamic Film Thickness in an Elliptical Contact. J. Lubr. Tech., Trans. ASME, series F, vol. 92, no. 1, Jan. 1970, pp. 155-162.
7. Ranger, A. P.: Numerical Solutions to the Elastohydrodynamic Equations. Ph. D. Dissertation, Dept. Mech. Eng., Imperial College of Sci. and Tech., March 1974.
8. Wedeven, L. D.; Evans, D.; and Cameron, A.: Optical Analysis of Ball Bearing Starvation. J. Lubr. Tech., Trans. ASME, series F., vol. 93, no. 3, July 1971, pp. 349-363.
9. Hamrock, Bernard J.; and Dowson, Duncan: Numerical Evaluation of the Surface Deformation of Elastic Solids Subjected to a Hertzian Contact Stress. NASA TN D-7774, 1974.
10. Roelands, C. J. A.: Correlational Aspects of the Viscosity-Temperature-Pressure Relationship of Lubricating Oils. Druk V. R. B., Groningen, Netherlands, 1966.
11. Harris, Tedric A.: Rolling Bearing Analysis. John Wiley & Sons, Inc., 1966.
12. Hamrock, Bernard J.; and Anderson, William J.: Arched-Outer-Race Ball-Bearing Considering Centrifugal Forces. NASA TN D-6765, 1972.
13. Snidle, R. W.; and Archard, J. F.: Lubrication at Elliptical Contacts. Paper 17, Inst. Mech. Eng. (London), 1969.
14. Dowson, D.; and Higginson, G. R.: Elastohydrodynamic Lubrication. Pergamon Press, 1966.

- 
15. Dowson, D.; and Whitaker, A. V.: A Numerical Procedure for the Solution of the Elastohydrodynamic Problems of Rolling and Sliding Contacts Lubricated by a Newtonian Fluid. Proc. Inst. Mech. Eng. (London), vol. 180, pt. 3B, 1965-1966, pp. 57-71.
 16. Whomes, T. L.: The Effect of Surface Quality on Lubricating Film Performance. Ph.D. Dissertation, Dept. Mech. Eng., University of Leeds, Oct. 1966.

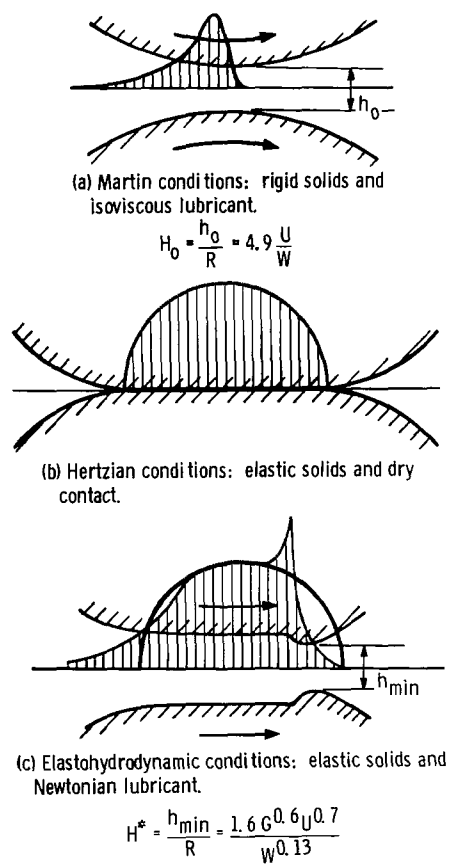


Figure 1. - Lubrication and contact conditions and minimum-film-thickness formulas.

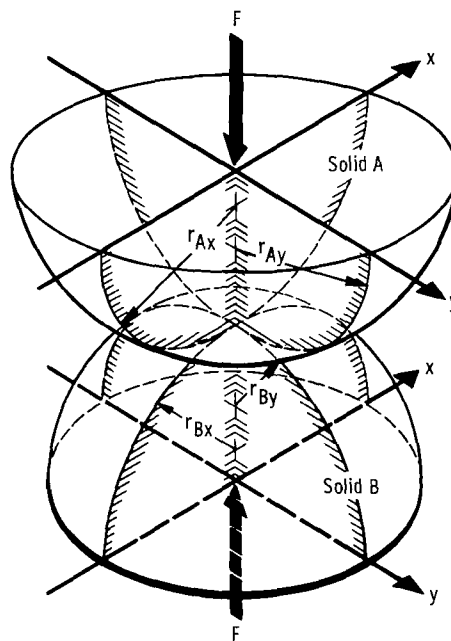


Figure 2. - Geometry of contacting elastic solids.

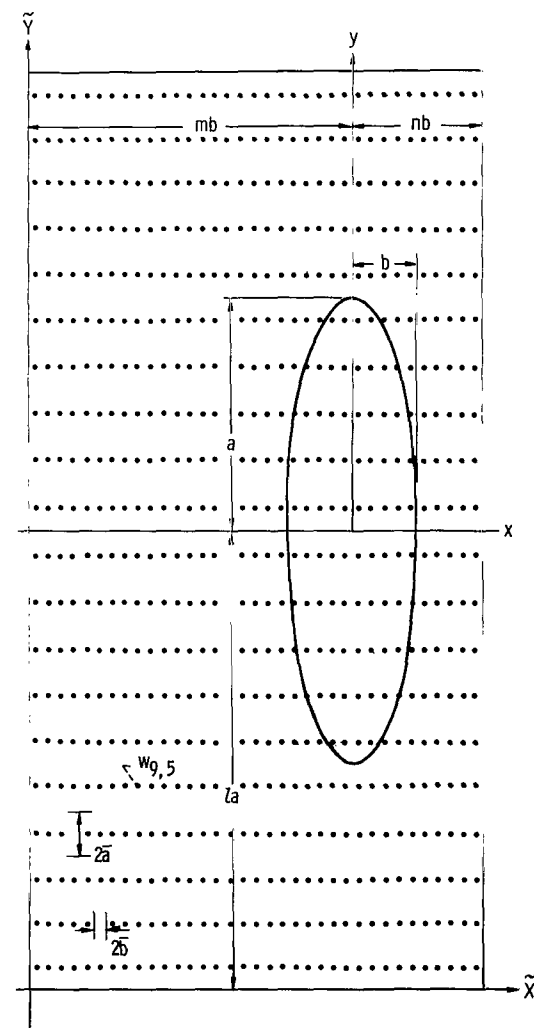


Figure 3. - Division of area in and around contact zone into equal rectangular areas.

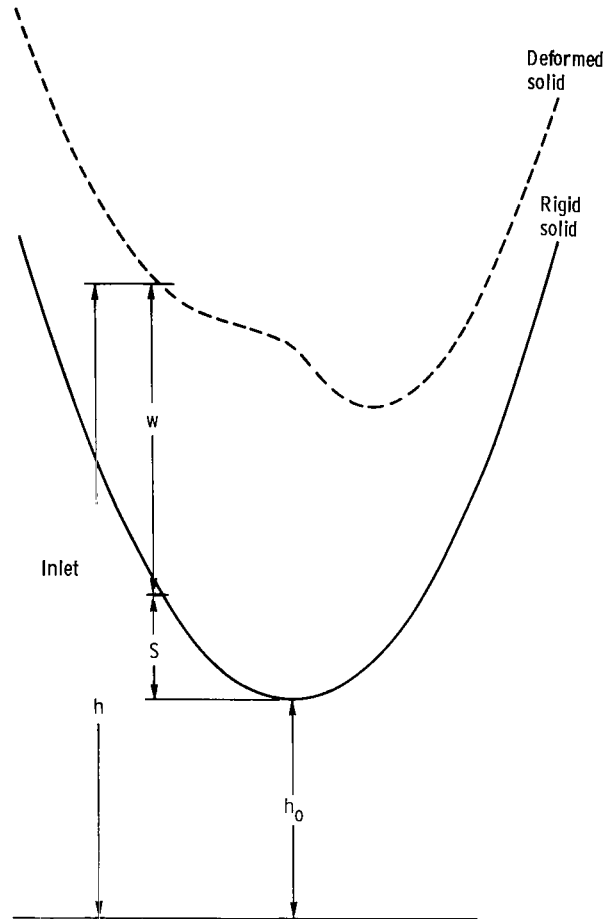


Figure 4. - Components of film thickness for ellipsoidal solid near a plane.

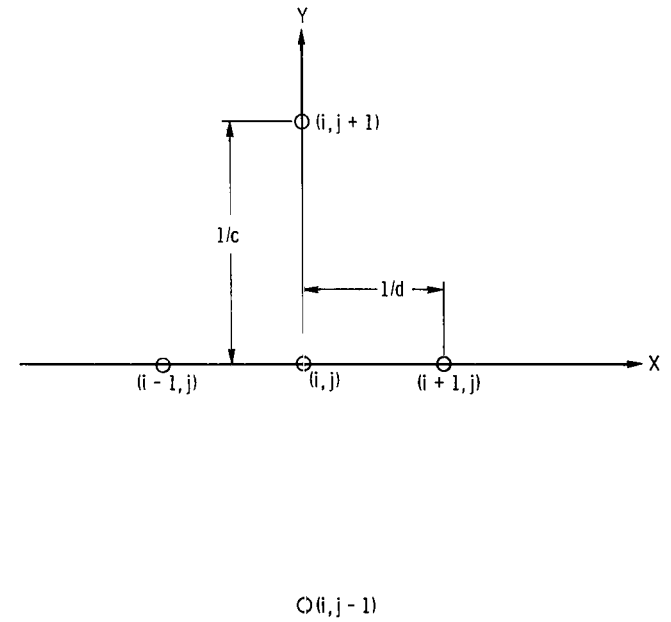


Figure 5. - Mesh used in numerical analysis.

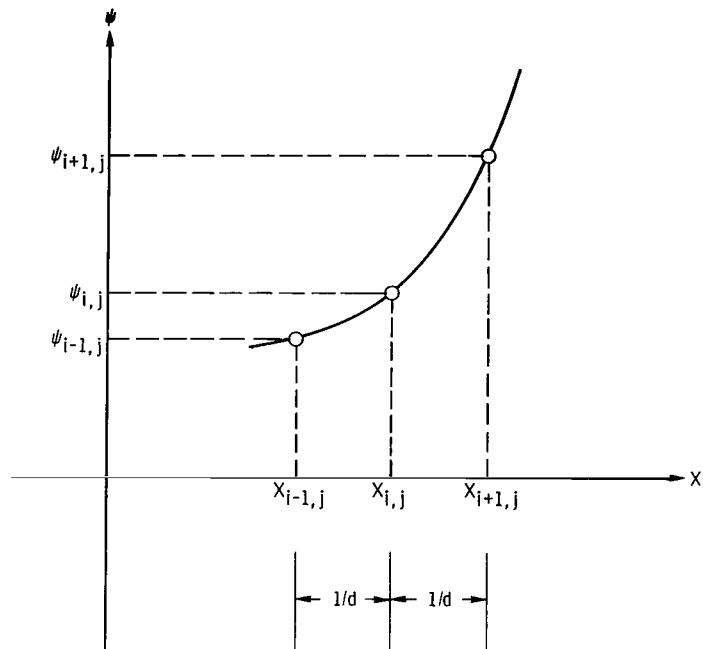


Figure 6. - Parabola and corresponding points representing ψ as a function of X .

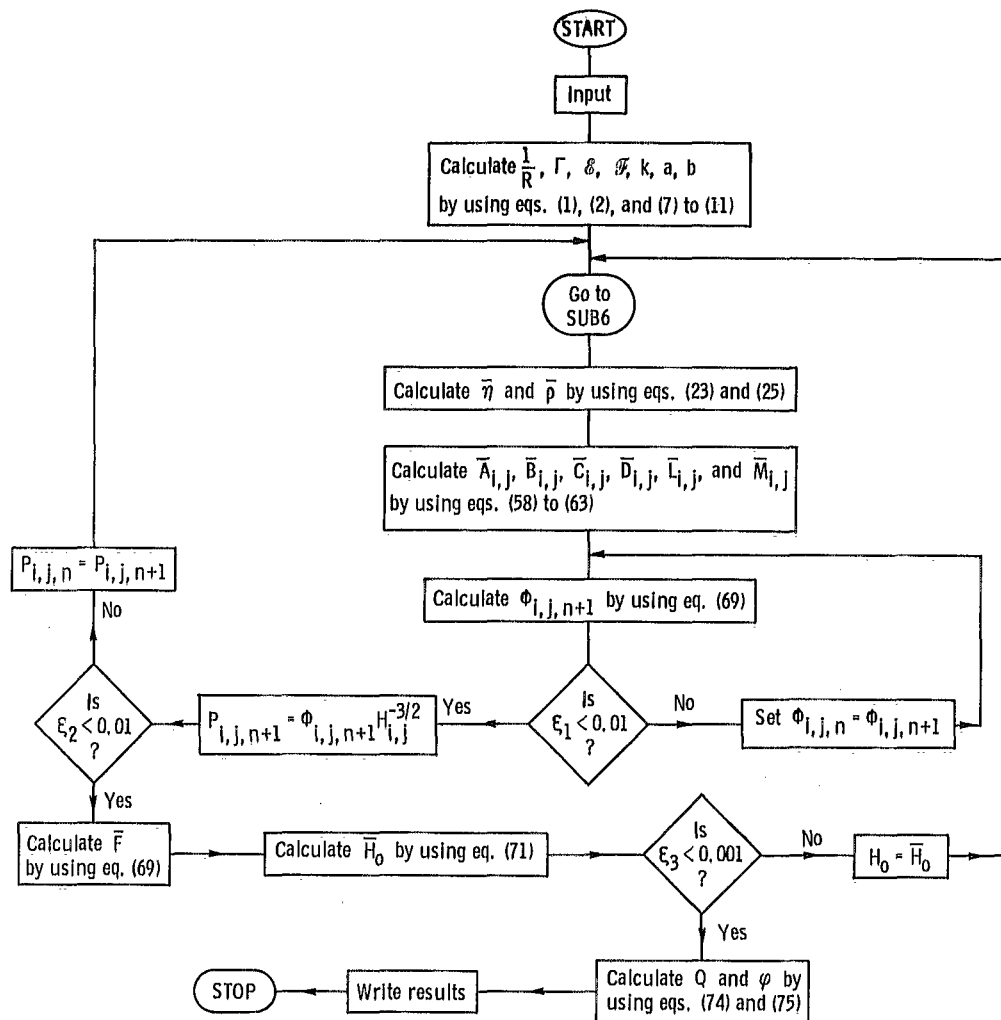


Figure 7. - Flow chart of main program.

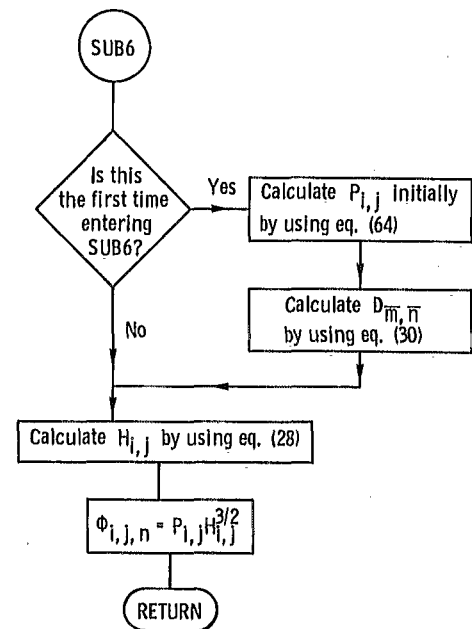


Figure 8. - Flow chart of subroutine SUB6.



834 001 C1 U D 750815 S00903DS
DEPT OF THE AIR FORCE
AF WEAPONS LABORATORY
ATTN: TECHNICAL LIBRARY (SUL)
KIRTLAND AFB NM 87117

POSTMASTER: If Undeliverable (Section 158
Postal Manual) Do Not Return

"The aeronautical and space activities of the United States shall be conducted so as to contribute . . . to the expansion of human knowledge of phenomena in the atmosphere and space. The Administration shall provide for the widest practicable and appropriate dissemination of information concerning its activities and the results thereof."

—NATIONAL AERONAUTICS AND SPACE ACT OF 1958

NASA SCIENTIFIC AND TECHNICAL PUBLICATIONS

TECHNICAL REPORTS: Scientific and technical information considered important, complete, and a lasting contribution to existing knowledge.

TECHNICAL NOTES: Information less broad in scope but nevertheless of importance as a contribution to existing knowledge.

TECHNICAL MEMORANDUMS: Information receiving limited distribution because of preliminary data, security classification, or other reasons. Also includes conference proceedings with either limited or unlimited distribution.

CONTRACTOR REPORTS: Scientific and technical information generated under a NASA contract or grant and considered an important contribution to existing knowledge.

TECHNICAL TRANSLATIONS: Information published in a foreign language considered to merit NASA distribution in English.

SPECIAL PUBLICATIONS: Information derived from or of value to NASA activities. Publications include final reports of major projects, monographs, data compilations, handbooks, sourcebooks, and special bibliographies.

TECHNOLOGY UTILIZATION PUBLICATIONS: Information on technology used by NASA that may be of particular interest in commercial and other non-aerospace applications. Publications include Tech Briefs, Technology Utilization Reports and Technology Surveys.

Details on the availability of these publications may be obtained from:

SCIENTIFIC AND TECHNICAL INFORMATION OFFICE

NATIONAL AERONAUTICS AND SPACE ADMINISTRATION

Washington, D.C. 20546